PERGAMON International Journal of Multiphase Flow 24 (1998) 775–792

International Journal of Multiphase Flow

Two-phase pressure drop and phase distribution at reduced tee junctions

L.C. Walters [a,*], H.M. Soliman [b], G.E. Sims [b]

[a] *Safety Thermalhydraulics Branch, AECL Research, Pinawa, Manitoba, Canada*
[b] *Department of Mechanical and Industrial Engineering, University of Manitoba, Winnipeg, Manitoba, Canada*

Received 22 November 1996; received in revised form 14 December 1997

Abstract

Experimental data are presented for the phase distribution and junction pressure drops of air–water mixtures (1.5 bar) in two reduced tee junctions. The junctions are horizontal with inlet and run diameters of 38.1 mm i.d. and branch diameters of 19.0 mm i.d. and 7.85 mm i.d. The tested range corresponds to inlet flow regimes of stratified, wavy and annular for both test sections plus slug for the larger-branch test section. Comparisons are made between the present data and existing models of pressure drop and phase distribution, thus identifying the models whose applicability can be extended to the present conditions.

Keywords: Pressure drop; Phase distribution; Reduced tee junctions; Experimental data

1. Introduction

As two-phase flow passes through dividing junctions, a maldistribution of the phases may occur where the qualities in the two legs downstream of the junction are not equal to the quality of the upstream flow. Understanding this phenomenon and the corresponding pressure distribution is necessary for the sake of design considerations in the power and process industries.

A review of the literature concerning two-phase flow mixtures through tee junctions reveals that a significant amount of recent research has been devoted to this problem. However, a general and effective model for predicting the distribution of the phases and the pressure drop has yet to be formulated. In order to support further the development of predictive models, a

* To whom correspondence should be addressed.

0301-9322/98/$19.00
PII: S0301-9322(98)00002-0

wide range of experimental data is necessary to aid researchers in accurately addressing the essential parameters such as the inlet quality, inlet mass flux, system pressure, inlet flow regime, extraction rate and branch orientation and size.

The amount of phase-distribution and pressure-drop data is limited for reduced tee junctions. Previous experimental data of phase separation obtained using reduced horizontal tee junctions include the studies by Collier (1976), Henry (1981), Shoham et al. (1989) and Azzopardi et al. (1988). The studies by Reimann et al. (1988), Ballyk et al. (1988) and Ballyk (1992) included both phase-distribution and pressure-drop data for reduced horizontal tee junctions.

The object of this investigation is to generate data concerning the effects of branch diameter on phase distribution and pressure drop for two-phase, air–water flow through horizontal tee junctions. This investigation includes two sets of data where the branch-to-inlet diameter ratio, D_3/D_1, was 0.206 and 0.5. Previous data taken in the same laboratory by Buell et al. (1994) with a diameter ratio of 1.0 allow for a comparison between the results for $D_3/D_1 = 0.206$, 0.5 and 1.0. The apparatus used to obtain these data was operated under the following conditions: air–water mixtures at a junction pressure of 150 ± 10 kPa abs and near-ambient temperature, inlet superficial gas velocities, J_{G1}, ranging between 2.7 and 40 m/s, inlet superficial liquid velocities, J_{L1}, ranging between 0.0021 and 0.181 m/s, and mass extraction rates, W_3/W_1, between 0 and 1.0, where W_1 and W_3 are the inlet and branch mass flow rates. Every attempt was made to impose the same operating conditions in the three data sets (corresponding to the three diameter ratios) in order to isolate the branch-diameter effect. The experimental data were then used in an examination of various phase-distribution and pressure-drop models.

2. Experimental investigation

2.1. Flow loop

The flow loop shown in Fig. 1, with the exception of the test section, is that used by Buell et al. (1994). Distilled water, stored in a water reservoir, was fed into the flow loop by a centrifugal pump. The water was filtered and metered before entering the mixer where it was mixed with the air. A cooling coil in the water reservoir removed the excess heat absorbed by the water due to flow through the pump and from frictional pressure losses. Air supplied from an air compressor was filtered, regulated and metered before entering the mixer. Exiting the mixer was a resultant two-phase, air–water mixture which was fed into the inlet side of the test section. All sides of the test section (the inlet side between the mixer and the tee junction and the two outlet sides, namely the run and the branch, from the tee junction to immediately before their respective separation tanks) were horiztontal. The inlet side was made of copper tubing of 38.1 mm i.d. and the first 67.5 tube diameters following the mixer were used for flow development. The two-phase mixture then entered a visual section of the same diameter where the inlet flow regime was observed. A further 41 tube diameters were allowed before the two-phase mixture entered the tee junction. The run also comprised 38.1 mm i.d. copper tubing with a total horizontal length of 97 diameters (including a visual section located 73 diameters from the tee junction) followed by a 90° elbow that directed the flow vertically downwards

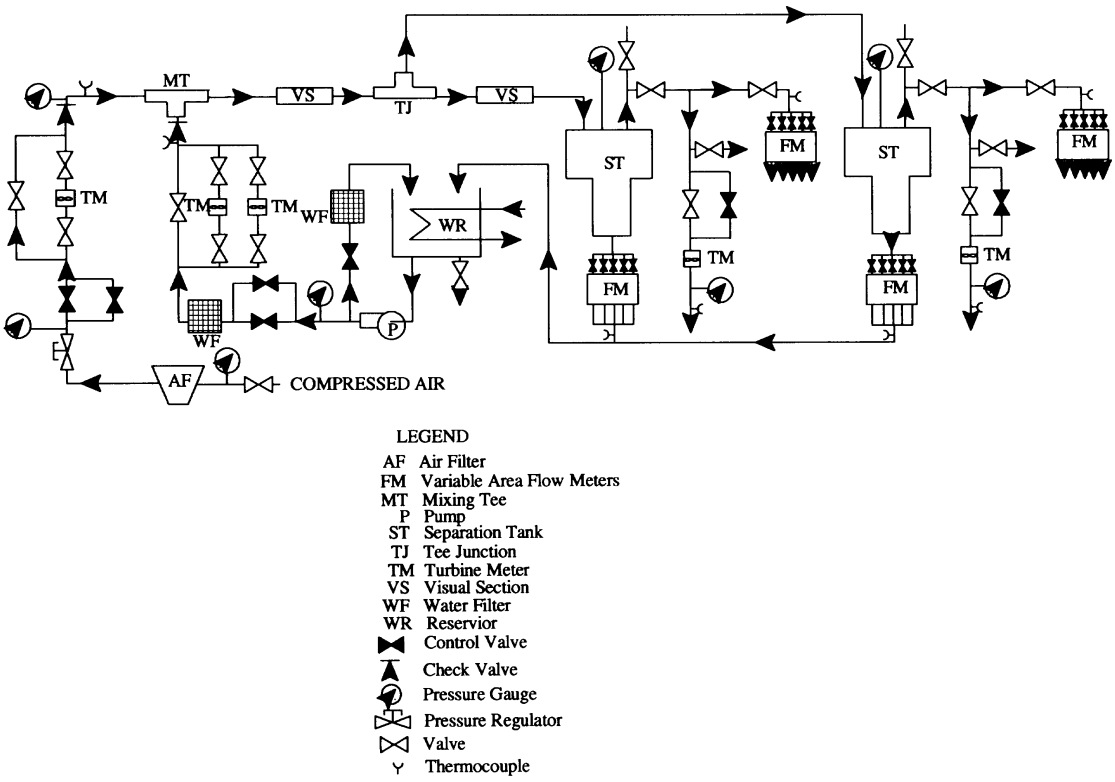

Fig. 1. Experimental test facility.

through a short section of tubing into the separation tank. The branch legs included copper tubing with 19.0 mm i.d. (for $D_3/D_1 = 0.5$) or 7.85 mm i.d. (for $D_3/D_1 = 0.206$) extending to a length of 1.47 m (for $D_3/D_1 = 0.5$) or 1.25 m (for $D_3/D_1 = 0.206$) from the tee junction, followed by a total horizontal length of 4.11 m (for $D_3/D_1 = 0.5$) or 4.31 m (for $D_3/D_1 = 0.206$) of 38.1 mm i.d. copper tubing, at which point a 90° elbow directed the flow vertically downwards through a short section of tubing into the separation tank. Air flows from both separation tanks were metered before being discharged to the atmosphere. Similarly, the liquid flow exiting each separation tank was metered before being returned back to the water reservoir.

In order to ensure consistency with other research laboratories, square-edged tee junctions (machined from brass blocks) were used. The main bodies of the tee junctions used in this investigation and the one used by Rubel et al. (1988) and Buell et al. (1994) were essentially identical, with the main difference being the diameter of the aperture leading to the branch. Detailed cross-sectional views of the tee junction can be found in Rubel et al. (1988) for the case of $D_3/D_1 = 1$ and $D_1 = 37.6$ mm.

Forty-one pressure taps were located along the test-section inlet, run and branch in order to measure the pressure distribution upstream and downstream of each tee junction. Each pressure tap on the inlet and run consisted of a 1.6 mm hole drilled through the tube wall. On the branch side, however, the size of the tap decreased with decreasing diameter. For the

branch diameters of 19 and 7.85 mm, the tap sizes were 1.25 and 1.02 mm, respectively. Clear plastic Tygon tubing pressure lines connected the pressure taps to the transducers.

2.2. Instrumentation

The inlet air mass flow rate, W_{G1}, was measured using a single turbine meter with a flow range of 0.14 to 4.53 m^3/min (air flow rates are quoted at standard conditions). The air mass flow rates exiting through the run, W_{G2}, and the branch, W_{G3}, were measured by a turbine meter at high flow rates (with a range equal to that of the inlet air turbine meter) or a bank of rotameters at low flow rates (with a range of 40 ml/min to 1235 l/min). The inlet water mass flow rate, W_{L1}, was measured using one of two turbine meters which were arranged in parallel and overlapped in range. The calibrated flow ranges of the turbine meters extended from 0.064 l/min to 18.9 l/min. The water mass flow rates in the run, W_{L2}, and branch, W_{L3}, were each metered using a separate bank of rotameters. The five rotameters in each bank were arranged in parallel to give a wide range of flow measurement from 2.2 ml/min to 13.7 l/min. Output from each turbine meter was converted to a 0–10 V DC signal and fed into the data-acquisition system. The average voltages from the turbine meters were obtained from samples taken over 30 s at a rate of 10 samples/s. Each instrument was regularly calibrated and good agreement, typically within $\pm 3\%$, was found between the calibrations and those provided by the manufacturer.

In order to measure the pressure distribution around the tee junction, two banks of differential pressure transducers were used. Each bank included three transducers with overlapping ranges covering an overall span of ± 57 cm water. One bank had an additional transducer (with a range of 0–1650 cm of water) to measure large pressure drops across the small branch. Output from the pressure transducers was in the form of a DC voltage signal (range ± 10 V) and was fed into the data-acquisition system. The average voltages from the transducers were then obtained from samples taken over 120 s at a rate of 100 samples/s. The appropriate calibration equations were then used to convert the average voltages into average differential pressures.

The data-acquisition system consisted of an 80286-based microcomputer with two plug-in analog-to-digital (A/D) boards. A computer program was used to control the gathering and reduction of data during experimental runs.

2.3. Data reduction

The mass flow rates W_{L1}, W_{G1}, W_{L2}, W_{G2}, W_{L3} and W_{G3} were calculated using the calibration curve of the appropriate device and the corresponding readings of pressure and/or temperature and were corrected for evaporation following the procedure outlined by Buell (1992). This procedure was used to correct flow rates for evaporation of the liquid phase in the mixer, test section and separation tanks. For $J_{G1} = 40$ m/s and $J_{L1} = 0.0021$ m/s, these corrections were found to be significant, with up to 20% of the water entering the mixer evaporating. At lower J_{G1} and higher J_{L1} these corrections were found to be insignificant.

Overall mass balances were performed individually on both the air and water streams. These errors are defined as the percentage deviation between the inlet flow rate of a specific phase

and the sum of its outlet flow rates from both separation tanks. For all test runs, the air mass-flow-rate balance was maintained within $\pm 6\%$, with 95% of the data for $D_3/D_1 = 0.5$ within $\pm 5\%$, and 98% of the data for $D_3/D_1 = 0.206$ within $\pm 5\%$. Similarly, the water mass-flow-rate balance was kept within $\pm 10\%$, with 89% of the data for $D_3/D_1 = 0.5$ within $\pm 5\%$, and 90% of the data for $D_3/D_1 = 0.206$ within $\pm 5\%$. The largest water mass balance errors occurred when evaporation was significant.

The junction pressure drops were determined by extrapolating the fully developed pressure gradients in the inlet, run and branch to the center of the tee junction. Linear equations were fitted to the fully developed data in the inlet, run and branch using the method of least squares. Details of the procedure followed in determining the inlet-to-run and inlet-to-branch pressure drops, ΔP_{12} and ΔP_{13}, respectively, can be found in Buell et al. (1994).

2.4. Experimental uncertainty

The experimental uncertainties for both test sections in the variables J_{G1}, J_{L1}, G_1 (inlet mass flux) and x_1 (inlet quality) were found to be within $\pm 5\%$. The uncertainty values for W_3/W_1 were within $\pm 23\%$. These values were large only when extraction rates were small (less than 0.1). For the branch-to-inlet quality ratio, x_3/x_1, the uncertainty was found to remain within $\pm 15\%$. For the fraction of liquid entering the branch, F_{BL}, the uncertainty was within $\pm 23\%$. It was found that the steadiness of the height of the gas–liquid interface in the branch separation tank is the dominant factor in the uncertainty for F_{BL}. Uncertainty values for very small F_{BL}s were not recorded since possible errors tended to be very large. For the fraction of gas entering the branch, F_{BG}, the uncertainty was found to remain within $\pm 15\%$. Finally, the uncertainties in the test section pressure, P_1, and temperature, T_1, were found to remain within $\pm 1.3\%$ and $\pm 0.3^{\circ}C$, respectively.

For $D_3/D_1 = 0.5$, it was found that approximately 80% of the uncertainty values for ΔP_{12} were within $\pm 20\%$ and 89% of the uncertainty values for ΔP_{13} were within $\pm 15\%$. Similarly, for $D_3/D_1 = 0.206$, approximately 82% of the uncertainty intervals for ΔP_{12} were found to be within $\pm 20\%$ and 86% of the uncertainty intervals for ΔP_{13} were within $\pm 15\%$. Uncertainty intervals for pressure drops less than 1 Pa were not reported since the possible errors could be very large on a percentage basis.

3. Results and discussion

3.1. Data range

For $D_3/D_1 = 0.5$, a total of 63 two-phase test runs were performed. These test runs constitute 15 different groups. Each group was characterized by fixed inlet conditions and variable extraction rates. The fixed inlet conditions included J_{G1}, J_{L1}, P_1, T_1 and inlet flow regime. Figure 2 shows the nominal values for J_{G1} and J_{L1} plotted on the Mandhane et al. (1974) flow-regime map. The actual values for J_{G1} and J_{L1} were maintained within $\pm 2\%$ of the average values of the group for over 96% of the test runs. The reduced experimental results for these runs are listed in Table 1.

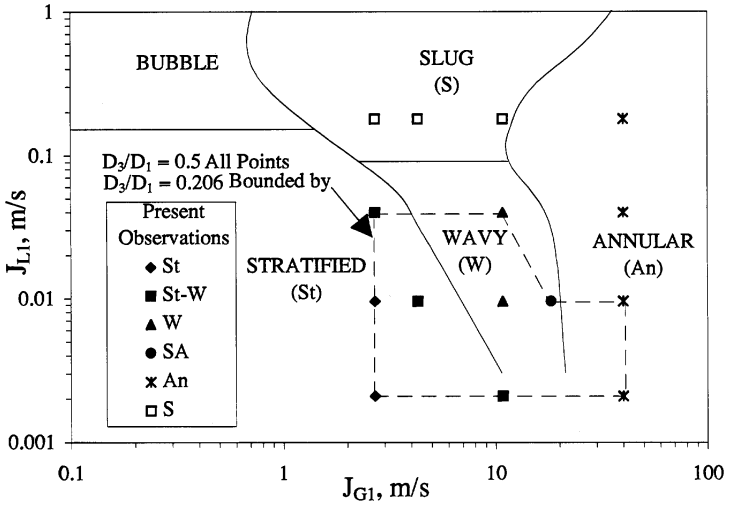

Fig. 2. Flow-regime map showing inlet conditions.

A total of 42 two-phase test runs were performed using $D_3/D_1 = 0.206$. These runs comprised 10 test groups, as shown on the Mandhane et al. (1974) flow-regime map in Fig. 2. Again, each group consisted of fixed inlet conditions (J_{G1}, J_{L1}, P_1, T_1 and inlet flow regime), and variable extraction rates. The actual values for J_{G1} and J_{L1} were maintained within $\pm 3\%$ of the average values of the group for over 97% of the test runs. The reduced experimental results for these runs are listed in Table 2.

The flow regimes observed in this investigation are consistent with the classifications shown on the map of Fig. 2. Identification of the major flow regimes was based on the standard descriptions (e.g. Mandhane et al., 1974) and the transitional flow regimes of stratified–wavy (St–W) and semi-annular (SA) were based on the descriptions of Buell et al. (1994).

Table 1
Pressure-drop and phase-distribution data for $D_3/D_1 = 0.5$

Test	J_{G1} (m/s)	J_{L1} (m/s)	P_1 (bar)	T_1 (°C)	x_1 (%)	W_3/W_1	x_3/x_1	ΔP_{21} (Pa)	ΔP_{13} (Pa)	Inlet flow regime
1-1	2.7	0.0021	1.49	18.7	69.0	0.100	1.43			Stratified
1-2	2.7	0.0022	1.50	20.0	69.6	0.301	1.42			
1-3	2.7	0.0021	1.51	18.9	69.3	0.498	1.43			
1-4	2.7	0.0021	1.50	19.5	69.4	0.700	1.34			
1-5	2.7	0.0021	1.51	18.4	69.3	0.750	1.32			
2-1	2.6	0.0092	1.50	20.4	33.5	0.103	2.96			Stratified
2-2	2.7	0.0092	1.50	20.9	34.3	0.303	2.22			
2-3	2.7	0.0092	1.50	21.4	33.8	0.501	1.80			
2-4	2.7	0.0094	1.50	20.3	33.7	0.555	1.80			
3-1	2.7	0.0387	1.51	21.0	10.9	0.103	2.55			Stratified-wavy
3-2	2.6	0.0387	1.51	20.8	10.8	0.300	1.70		55	
3-3	2.6	0.0387	1.51	20.9	10.7	0.497	1.80	12	156	
3-4	2.6	0.0388	1.52	21.1	10.7	0.530	1.86	14	187	

4-1	2.7	0.1806	1.51	21.2	2.6	0.100	7.88	119	184	Slug
4-2	2.7	0.1805	1.50	21.2	2.6	0.298	3.00	129	550	
4-3	2.7	0.1800	1.50	21.1	2.6	0.498	1.96	133	1303	
4-4	2.7	0.1796	1.49	21.2	2.6	0.660	1.42		3207	
5-1	4.3	0.0095	1.50	20.6	44.9	0.100	2.21	12		Stratified-wavy
5-2	4.4	0.0096	1.51	19.8	45.2	0.302	1.62		82	
5-3	4.4	0.0096	1.51	20.1	45.0	0.501	1.32		166	
5-4	4.4	0.0096	1.49	18.6	44.8	0.700	1.18		275	
5-5	4.4	0.0095	1.51	18.5	45.1	0.844	1.19		380	
6-1	4.3	0.1806	1.50	21.1	4.0	0.103	6.53	95	246	Slug
6-2	4.3	0.1820	1.50	21.1	4.0	0.297	3.12	168	963	
6-3	4.3	0.1819	1.49	21.1	4.0	0.504	1.93	243	1276	
6-4	4.3	0.1811	1.51	21.1	4.0	0.685	1.45			
7-1	10.7	0.0021	1.50	14.4	90.1	0.099	1.10	16		Stratified-wavy
7-2	10.6	0.0021	1.50	16.5	90.1	0.301	0.97	54	127	
7-3	10.6	0.0021	1.50	16.9	90.0	0.499	0.90	71	414	
7-4	10.6	0.0021	1.51	14.3	90.2	0.700	0.95		1147	
7-5	10.5	0.0021	1.50	14.5	89.9	0.905	0.99		1840	
8-1	10.4	0.0095	1.50	18.2	66.3	0.099	1.49	29	-29	Wavy
8-2	10.5	0.0096	1.50	19.0	66.2	0.299	1.32	83	271	
8-3	10.4	0.0095	1.50	18.3	66.2	0.501	1.10	89	659	
8-4	10.4	0.0094	1.50	18.2	66.3	0.698	1.04	100	1226	
8-5	10.4	0.0092	1.51	18.2	67.0	0.900	0.99	98	2012	
9-1	10.5	0.0389	1.51	20.1	32.6	0.100	2.74	89	125	Wavy
9-2	10.6	0.0392	1.50	19.9	32.2	0.300	2.30	160	1195	
9-3	10.8	0.0409	1.51	20.6	32.1	0.499	1.83	193	3094	
9-4	10.8	0.0404	1.51	20.1	32.4	0.651	1.59	179	3509	
10-1	10.8	0.1808	1.50	21.0	9.6	0.101	4.61	216	783	Slug
10-2	10.8	0.1810	1.50	20.8	9.6	0.295	3.40	329	4188	
10-3	10.7	0.1811	1.51	21.2	9.5	0.510	1.96		5954	
10-4	10.8	0.1813	1.51	21.2	9.5	0.611	1.63		6573	
11-1	18.2	0.0096	1.50	16.9	77.3	0.100	1.13	88	4	Semi-annular
11-2	18.3	0.0095	1.50	16.4	77.6	0.297	1.11	178	879	
11-3	18.2	0.0096	1.50	16.7	77.5	0.500	1.05	234	2142	
11-4	18.3	0.0095	1.50	15.9	77.6	0.698	1.03	256	4044	
11-5	18.2	0.0096	1.50	15.8	77.4	0.903	0.99	242	6415	
12-1	40.7	0.0021	1.50	14.2	97.2	0.099	0.98	374	176	Annular
12-2	40.5	0.0021	1.50	14.0	97.2	0.298	0.95	798	3754	
12-3	40.1	0.0021	1.50	14.0	97.2	0.499	0.97	1004	8263	
12-4	40.4	0.0022	1.50	14.2	97.1	0.624	0.98	1031	13 616	
13-1	39.8	0.0095	1.51	14.3	88.4	0.101	0.88	311	253	Annular
13-2	39.8	0.0096	1.50	15.2	88.2	0.305	0.92	830	3135	
13-3	39.8	0.0096	1.50	14.7	88.3	0.504	0.90	1051	8281	
13-4	40.0	0.0095	1.50	14.6	88.4	0.607	0.92	1150	13 553	
14-1	40.5	0.0398	1.50	16.6	64.7	0.100	0.86	374	371	Annular
14-2	39.9	0.0397	1.50	17.1	64.3	0.301	1.07	1067	5120	
14-3	39.6	0.0397	1.50	16.7	64.1	0.480	1.08	1322	13 819	
15-1	40.2	0.1808	1.50	15.8	28.6	0.164	1.91	1688	6104	Annular
15-2	40.1	0.1806	1.49	15.6	28.4	0.202	1.91	1882	9302	
15-3	40.5	0.1805	1.48	15.4	28.6	0.233	1.87	1996	13 040	

Table 2
Pressure-drop and phase-distribution data for $D_3/D_1 = 0.206$

Test	J_{G1} (m/s)	J_{L1} (m/s)	P_1 (bar)	T_1 (°C)	x_1 (%)	W_3/W_1	x_3/x_1	ΔP_{21} (Pa)	ΔP_{13} (Pa)	Inlet flow regime
16-1	2.7	0.0021	1.50	18.4	69.5	0.100	1.43	3	107	Stratified
16-2	2.7	0.0021	1.50	19.1	69.6	0.300	1.43	8	1056	
16-3	2.7	0.0021	1.50	18.3	69.5	0.495	1.06	9	1734	
16-4	2.7	0.0021	1.50	18.3	69.5	0.700	0.83	10	2048	
16-5	2.7	0.0022	1.50	18.2	69.1	0.899	0.95	8	3516	
17-1	2.7	0.0095	1.50	20.6	33.5	0.100	2.98	6	438	Stratified
17-2	2.7	0.0095	1.50	21.4	33.3	0.300	1.69	9	854	
17-3	2.7	0.0095	1.50	21.1	33.7	0.496	1.21	10	2126	
17-4	2.7	0.0095	1.49	21.2	33.3	0.703	0.95	9	2512	
17-5	2.7	0.0095	1.50	22.0	33.4	0.806	0.99	9	3231	
18-1	2.7	0.0398	1.50	21.6	10.7	0.050	3.18	6	108	Stratified-wavy
18-2	2.7	0.0397	1.50	21.2	10.8	0.100	2.18	7	272	
18-3	2.7	0.0399	1.50	21.2	10.7	0.300	1.26	11	1090	
18-4	2.7	0.0397	1.50	21.2	10.7	0.502	1.07	13	2530	
19-1	4.3	0.0095	1.50	21.8	44.4	0.101	2.25	11	714	Stratified-wavy
19-2	4.3	0.0095	1.50	20.4	44.5	0.305	1.78	17	2758	
19-3	4.3	0.0096	1.51	20.6	44.6	0.502	1.26	19	4200	
19-4	4.3	0.0095	1.50	21.2	44.8	0.601	1.05	18	4766	
20-1	10.8	0.0021	1.51	15.7	90.1	0.050	1.10	10	256	Stratified-wavy
20-2	10.8	0.0021	1.50	15.2	90.0	0.100	1.10	29	1150	
20-3	10.8	0.0021	1.50	16.1	90.2	0.300	0.97	58	8716	
20-4	10.8	0.0022	1.50	15.9	90.0	0.345	0.96	61	9656	
21-1	10.8	0.0095	1.51	19.5	67.1	0.050	1.49	18	447	Wavy
21-2	10.8	0.0095	1.51	19.5	67.0	0.100	1.49	24	1095	
21-3	10.8	0.0094	1.51	19.3	67.2	0.199	1.42	53	5791	
21-4	10.8	0.0094	1.51	19.2	67.2	0.272	1.40	70	11915	
22-1	10.8	0.0396	1.49	20.6	32.5	0.025	2.57	19	347	Wavy
22-2	10.8	0.0397	1.50	20.4	32.5	0.050	2.69	28	1831	
22-3	10.8	0.0398	1.50	20.6	32.5	0.100	2.77	49	5585	
22-4	10.8	0.0397	1.50	21.4	32.5	0.133	2.75	68	10690	
23-1	18.3	0.0094	1.50	17.2	77.6	0.051	1.13	54	816	Semi-annular
23-2	18.3	0.0094	1.50	17.4	77.7	0.100	1.16	86	3098	
23-3	18.3	0.0095	1.50	17.5	77.6	0.150	1.15	116	8049	
23-4	18.3	0.0095	1.50	16.5	77.7	0.185	1.16	126	10064	
24-1	40.2	0.0020	1.50	14.7	97.3	0.025	0.94	100	620	Annular
24-2	40.3	0.0020	1.50	15.2	97.3	0.050	0.95	189	3187	
24-3	40.0	0.0021	1.51	14.8	97.2	0.075	0.96	273	7403	
24-4	40.1	0.0021	1.50	14.4	97.1	0.096	0.96	333	11767	
25-1	40.0	0.0094	1.51	15.4	88.5	0.031	0.63	119	541	Annular
25-2	40.0	0.0095	1.51	15.6	88.4	0.050	0.75	184	1623	
25-3	40.2	0.0095	1.50	15.6	88.4	0.075	0.81	277	5760	
25-4	40.1	0.0095	1.50	15.4	88.4	0.101	0.83	352	10 280	

3.2. Phase distribution data

3.2.1. Present data

It was found that for $D_3/D_1 = 0.5$ most of the stratified, stratified–wavy, wavy and semi-annular data show a preference for the gas phase to exit through the branch. These trends are well represented by the data in Fig. 3, where an increase in J_{G1} is associated with more liquid entering the branch. Figure 4 shows that the slug-flow data displayed a strong preference for the gas phase to exit through the branch particularly for larger extraction rates. The annular flow data showed large variations in the distribution of the phases depending on J_{L1}. Figure 5 shows that as J_{L1} increases, less liquid will exit through the branch. Azzopardi et al. (1988) suggested that for annular flow an increase in the liquid flow rate would increase the amount of liquid entrainment. This would decrease the fraction of liquid in the film, which is the major source of liquid in the branch. Therefore, the fraction of liquid entering the branch would decrease.

For $D_3/D_1 = 0.206$, the stratified, stratified–wavy, wavy and semi-annular data showed a preference for the gas phase to exit through the branch at low extraction rates, as shown in Fig. 6. Where larger extraction rates could be obtained, the data tend to show an increased fraction of liquid is diverted towards the branch. Other data and analysis can be found in Walters (1994).

3.2.2. Comparison with other data

Azzopardi et al. (1988) obtained air–water, phase-separation data in the stratified, wavy and annular flow regimes. Figure 7 shows a comparison between the present study for $D_3/D_1 = 0.5$ and the Azzopardi et al. (1988) wavy data for $D_3/D_1 = 0.67$. Similar system pressure (1.5 bar) was used in both sets of data. The agreement appears to be quite good, when values of J_{L1} and J_{G1} are matched fairly well between the two studies. Other comparisons (with good agreement) can be found in Walters (1994).

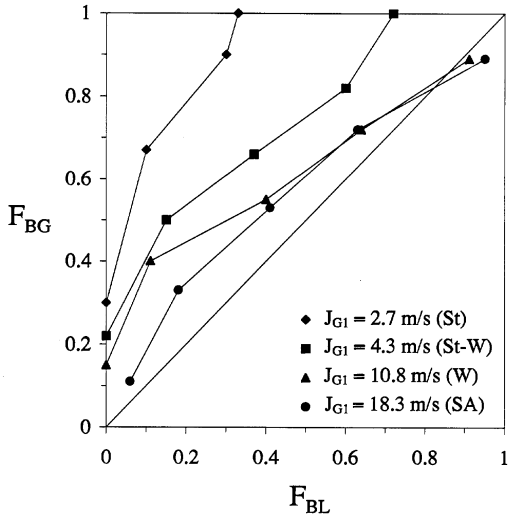

Fig. 3. Phase-separation data for $J_{L1} = 0.0095$ m/s and $D_3/D_1 = 0.5$.

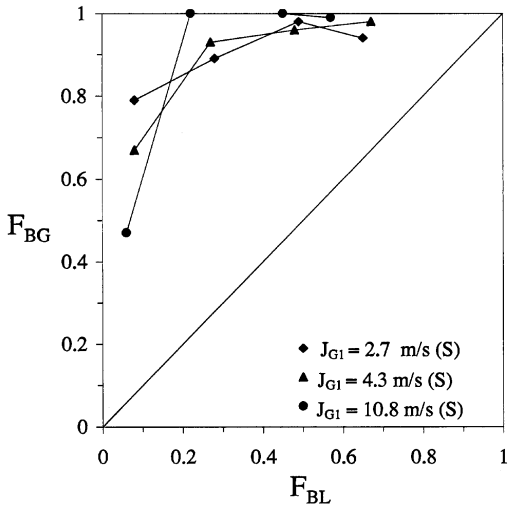

Fig. 4. Phase-separation data for $J_{L1} = 0.180$ m/s and $D_3/D_1 = 0.5$.

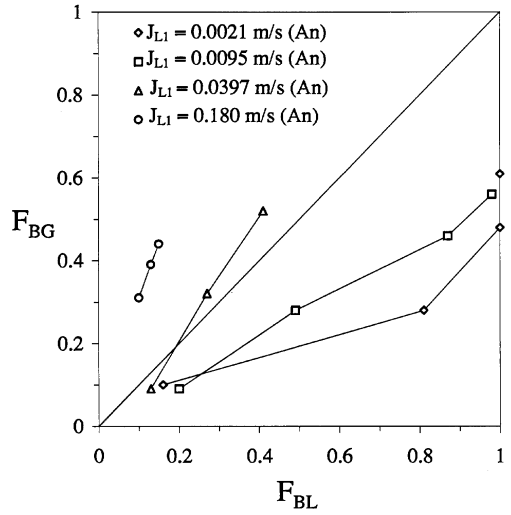

Fig. 5. Phase-separation data for $J_{G1} = 40$ m/s and $D_3/D_1 = 0.5$.

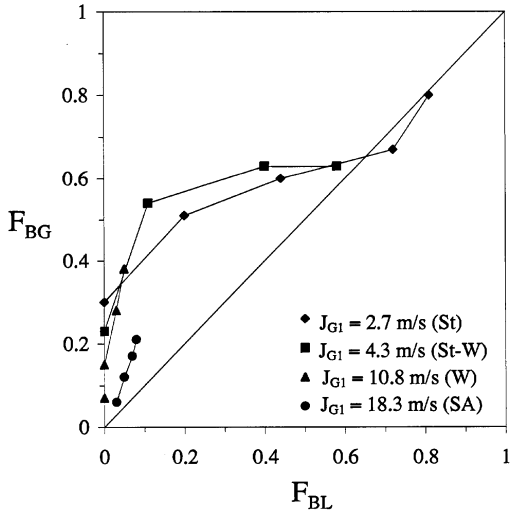

Fig. 6. Phase-separation data for $J_{L1} = 0.0095$ m/s and $D_3/D_1 = 0.206$.

3.2.3. The effect of diameter ratio

Data in the stratified flow regime (Fig. 8) show that for $D_3/D_1 = 0.5$ the gas phase has a greater tendency to enter the branch than when $D_3/D_1 = 1.0$. Intuitively, it is reasonable to expect that a smaller fraction of the liquid could be taken off into the branch as the branch diameter decreases since the liquid flowing along the bottom of the main tube would have to climb the wall before exiting through the branch (Shoham et al., 1989).

However, the trend for $D_3/D_1 = 0.206$ is not as consistent. At low extraction rates, the phase distribution data are very similar to those of $D_3/D_1 = 0.5$. As the extraction rate increases, the

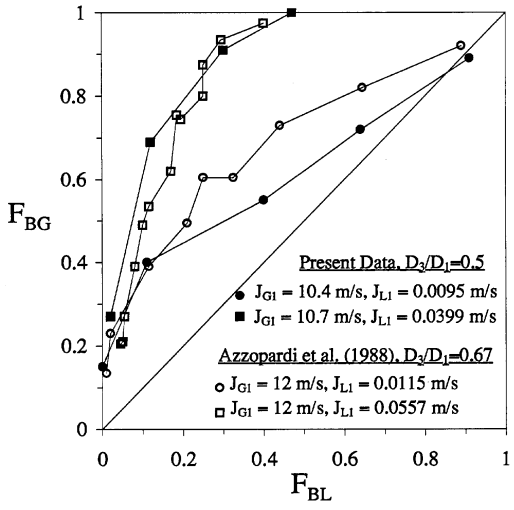

Fig. 7. Comparison between the present data and Azzopardi et al. (1988).

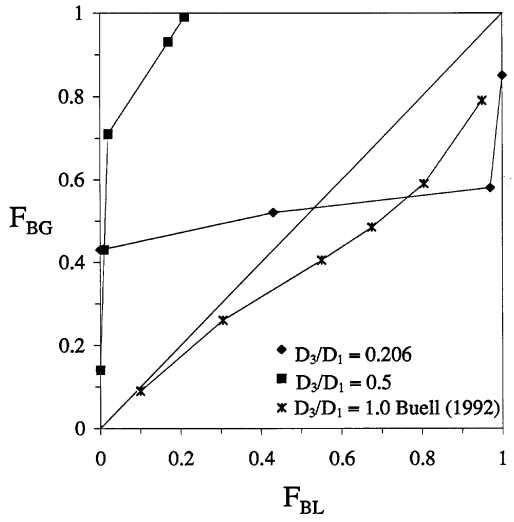

Fig. 8. Effect of diameter ratio at $J_{L1} = 0.0021$ m/s and $J_{G1} = 2.7$ m/s.

tendency for liquid preferentially to enter the branch begins to increase and the phase distribution data approach the case of $D_3/D_1 = 1.0$. A possible explanation for this phenomenon may relate to the fact that the area of the branch for $D_3/D_1 = 0.206$ is much smaller than that of $D_3/D_1 = 0.5$, and therefore for similar values of F_{BG}, J_{G3} for $D_3/D_1 = 0.206$ is considerably larger than J_{G3} for $D_3/D_1 = 0.5$. Due to a Bernoulli effect, it is possible that liquid entrainment into the branch is responsible for this phenomenon.

While only data in the stratified flow regime have been presented, these trends are consistent in the stratified–wavy, wavy, semi-annular and annular flow regimes. However, for $D_3/D_1 = 0.206$, large extraction rates were not always attainable and therefore assessment of trends did not always cover the whole range of extraction rates (Walters, 1994).

3.2.4. Comparison with models

The present experimental data (values of x_3/x_1 at given values of W_3/W_1) were compared against the existing phase-distribution models of Hwang et al. (1988), Hart et al. (1991), Azzopardi (1988) and Shoham et al. (1987). Tables 3 and 4 show a summary of the performance of the phase-distribution models for $D_3/D_1 = 0.5$ and 0.206, respectively. For annular flow, it was found that the geometrically based model by Azzopardi (1988), using the correlation of Kataoka and Ishii (1983) for entrainment, gave the best results for both diameter ratios. For $D_3/D_1 = 0.5$, the Azzopardi (1988) model predicted 79% of the annular data within $\pm 20\%$ and for $D_3/D_1 = 0.206$, all the data were predicted within $\pm 20\%$. The model by Hart et al. (1991) also gave good results for the stratified, wavy and annular flow regimes with 88% of the data for $D_3/D_1 = 0.5$ predicted within $\pm 20\%$ and 64% of the data for $D_3/D_1 = 0.206$ predicted within $\pm 20\%$. However, this model is limited to liquid holdups less than

Table 3
Summary of the performance of phase-distribution models, $D_3/D_1 = 0.5$

Model[a]	Interval (%)	Data predicted correctly (%)	Arithmetic mean deviation (%)	rms deviation (%)
HWM1	±50	100		
	±20	46	−23.3	29.5
HWM2	±50	64		
	±20	36	−36.3	47.2
HWM3	±50	50		
	±20	8	−50.3	53.8
AM	±50	100		
	±20	79	−5.2	14.7
HM	±50	91		
	±20	88	+9.0	27.5
SM	±50	100		
	±20	71	−14.1	23.6

[a] HWM1 = model by Hwang et al. (1988), stratified and wavy flow regimes; HWM2 = model by Hwang et al. (1988), annular flow regime; HWM3 = model by Hwang et al. (1988), slug flow regime; AM = model by Azzopardi (1988), annular flow regime; HM = model by Hart et al. (1991), stratified, wavy and annular flow regimes and liquid holdup less then 0.06; SM = model by Shoham et al. (1987), annular flow regime.

Table 4
Summary of the performance of phase-distribution models, $D_3/D_1 = 0.206$

Model[a]	Interval (%)	Data predicted correctly (%)	Arithmetic mean deviation (%)	rms deviation (%)
HWM1	±50	100		
	±20	65	−12.9	21.1
HWM2	±50	25		
	±20	0	−77.8	82.9
AM	±50	100		
	±20	100	+5.2	7.6
HM	±50	96		
	±20	64	−5.5	21.6

[a] HWM1 = model by Hwang et al. (1988), stratified and wavy flow regimes; HWM2 = model by Hwang et al. (1988), annular flow regime; AM = model by Azzopardi (1988), annular flow regime; HM = model by Hart et al. (1991), stratified, wavy and annular flow regimes and liquid holdup less then 0.06.

0.06. Typically, the deviation between the data and any of the models is highest at low extraction rates and this deviation decreases as the extraction rate increases.

3.3. Pressure-drop data

3.3.1. Single-phase flow

Based on a simple one-dimensional momentum balance for the tee junction, Collier (1976) presented a model for the pressure drop ΔP_{12}, whereby

$$\Delta P_{12} = P_1 - P_2 = K_{12}(G_2^2 - G_1^2)/\rho, \tag{1}$$

where K_{12} is the momentum correction factor, ρ is the density, P_1 and P_2 are the average pressures on the inlet and run sides, respectively, and G_1 and G_2 are the inlet and run mass fluxes, respectively.

Alternatively, ΔP_{13}, can be modeled using reversible and irreversible components:

$$\Delta P_{13} = P_1 - P_3 = (\Delta P_{13})_{\mathrm{REV}} + (\Delta P_{13})_{\mathrm{IRR}}, \tag{2}$$

where

$$(\Delta P_{13})_{\mathrm{REV}} = (G_3^2 - G_1^2)/(2\rho), \tag{3}$$

$$(\Delta P_{13})_{\mathrm{IRR}} = K_{13}G_1^2/(2\rho), \tag{4}$$

G_3 is the branch mass flux, P_3 is the average pressure on the branch side of the junction and K_{13} is the single-phase loss coefficient through the branch.

Seven single-phase (water) runs were performed with each test section. These test runs were carried out at an inlet liquid velocity of 0.180 m/s (±0.5%). Apart from the diameter ratio, the only parameter varied was the extraction rate. For both test sections, the single-phase pressure drop data were used to calculate K_{12} and K_{13} and empirical equations were developed for both parameters (Walters, 1994).

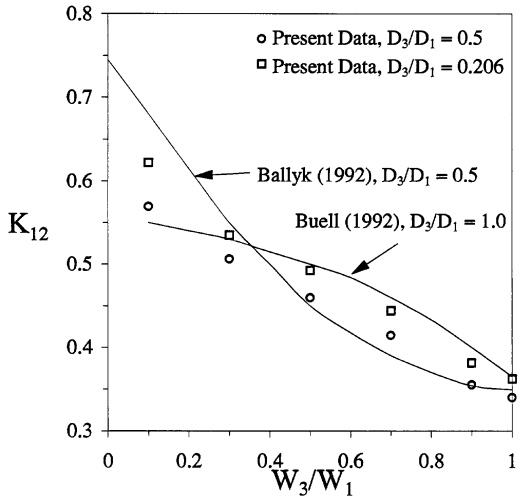

Fig. 9. Momentum correction factors, K_{12}.

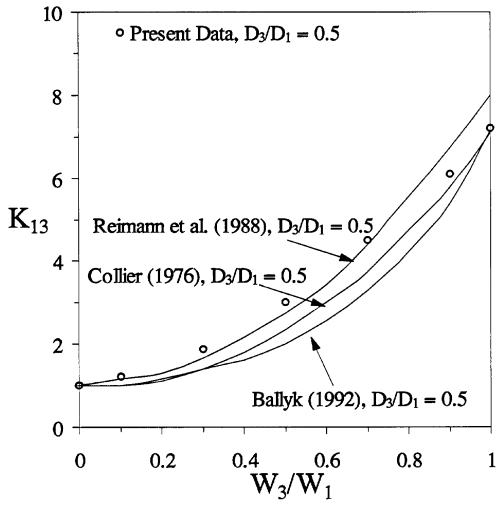

Fig. 10. Loss coefficient, K_{13}, for $D_3/D_1 = 0.5$.

Figure 9 shows that the agreement between the present data for K_{12} and the empirical equation provided by Ballyk (1992) is good, especially at high extraction rates. This figure also shows that the effect of D_3/D_1 on K_{12} is small.

Existing correlations and present data for K_{13} for $D_3/D_1 = 0.5$ and 0.206 are shown in Figs. 10 and 11, respectively. Agreement among data and correlations is quite good for both test sections. Figures 10 and 11 show that D_3/D_1 has a strong effect on K_{13} and consequently ΔP_{13}.

3.3.2. Two-phase flow

A sample of the results for ΔP_{12} and ΔP_{13} is shown in Figs. 12 and 13, respectively. These

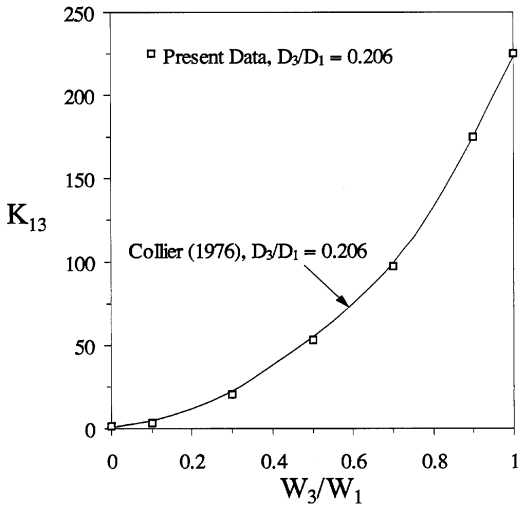

Fig. 11. Loss coefficient, K_{13}, for $D_3/D_1 = 0.206$.

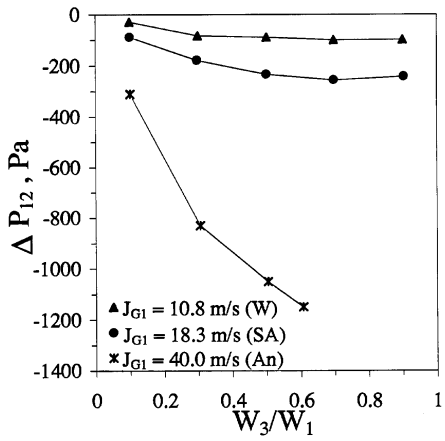

Fig. 12. Pressure drop ΔP_{12} for $J_{L1} = 0.0095$ m/s and $D_3/D_1 = 0.5$.

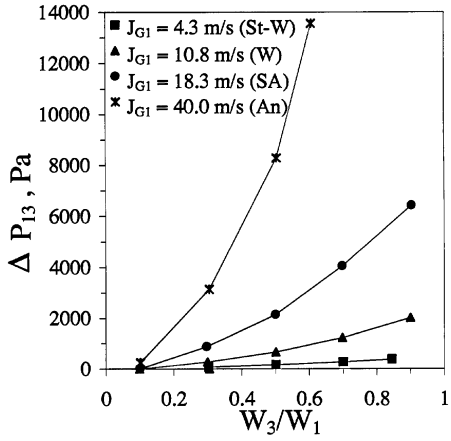

Fig. 13. Pressure drop ΔP_{13} for $J_{L1} = 0.0095$ m/s and $D_3/D_1 = 0.5$.

results demonstrate the effects of W_3/W_1 and J_{G1} on the two pressure drops for fixed values of J_{L1} and D_3/D_1. The general trend is that the absolute values of ΔP_{12} and ΔP_{13} increase monotonically with J_{G1}. The value of ΔP_{13} increases continuously with W_3/W_1, while for the cases where ΔP_{21} was measured over the whole range of W_3/W_1, the value of ΔP_{21} increases at first with W_3/W_1, but becomes essentially independent of W_3/W_1 at higher extraction rates (the value of W_3/W_1 at which this occurs appears to depend on the inlet conditions).

The effect of D_3/D_1 on the two-phase pressure drops is demonstrated in Figs. 14 and 15. While these results correspond to a given combination of J_{L1} and J_{G1}, the displayed trend is typical of all inlet conditions. Figure 14 shows that the effect of D_3/D_1 on ΔP_{12} is minimal. On the other hand, ΔP_{13} increases significantly with a decrease in D_3/D_1. These results are consistent with the single-phase results shown earlier in Figs. 9–11.

The pressure-drop data (ΔP_{12} and ΔP_{13}) for both diameter ratios used in this investigation were compared against pressure-drop models existing in the literature. The models tested were

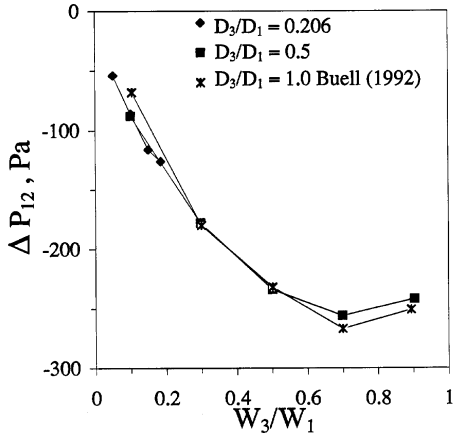

Fig. 14. Pressure drop ΔP_{12} for $J_{L1} = 0.0095$ m/s and $J_{G1} = 18.3$ m/s.

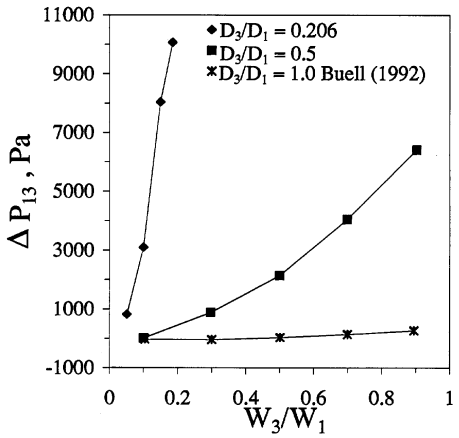

Fig. 15. Pressure drop ΔP_{13} for $J_{L1} = 0.0095$ m/s and $J_{G1} = 18.3$ m/s.

the homogeneous flow model by Saba and Lahey (1984), the separated flow model by Fouda and Rhodes (1974), the model by Reimann and Seeger (1986) and the model by Hwang and Lahey (1988). A summary of the equations used in these models was given by Buell et al. (1994).

Table 5 summarizes the performance of the various ΔP_{12} models for both branch-to-inlet diameter ratios. The separated flow model (SFM) has the best overall predictive capabilities and the lowest deviations for both diameter ratios. This model tends to underpredict slightly the measured data, especially for the slug-flow regime ($D_3/D_1 = 0.5$ only). The model by Hwang and Lahey (1988) tended to underpredict most of the data with mass extraction rates less than 0.2. Otherwise this model tended to predict accurately the present data for extraction rates higher than 0.2. The suggestion by Hwang and Lahey (1988) of using the Zuber and Findlay (1965) model to calculate the void fraction gave better results than when the Rouhani (1969) correlation was used.

Table 6 summarizes the performance of the various ΔP_{13} models. For both diameter ratios, the separated flow model (SFM) gave the best overall predictions and the lowest deviations.

Table 5
Summary of the performance of ΔP_{12} models

			Data predicted correctly (%)				Deviation (%)	
			Inlet flow regime					
Model[a]	D_3/D_1	Interval (%)	St, W St–W	S	SA An	Overall	Arithmetic mean	rms
HFM	0.206	±50	53	—	92	64	+58.3	96.2
		±30	30	—	42	33		
	0.5	±50	60	0	95	64	+56.5	99.2
		±30	40	0	84	52		
SFM	0.206	±50	90	—	83	88	−3.9	37.7
		±30	50	—	58	52		
	0.5	±50	93	88	95	93	−19.8	30.2
		±30	73	13	79	67		
RSM	0.206	±50	57	—	50	55	+107.3	221.3
		±30	23	—	50	31		
	0.5	±50	60	38	84	67	+27.8	57.5
		±30	47	38	74	57		
HLM1	0.206	±50	37	—	50	40	−128.2	239.3
		±30	17	—	42	24		
	0.5	±50	60	75	63	64	−35.5	78.0
		±30	40	38	58	48		
HLM2	0.206	±50	33	—	33	33	−151.5	276.7
		±30	17	—	17	17		
	0.5	±50	67	50	63	62	−59.5	87.6
		±30	53	13	58	48		

[a] HFM = homogeneous flow model, SFM = separated flow model, RSM = Reimann and Seeger (1986) model, HLM1 = Hwang and Lahey (1988) model with α_1 calculated using the Zuber and Findlay (1965) model, HLM2 = Hwang and Lahey (1988) model with α_1 calculated using the Rouhani (1969) correlation.

Table 6
Summary of the performance of ΔP_{13} models

			Data predicted correctly (%)				Deviation (%)	
			Inlet flow regime					
Model[a]	D_3/D_1	Interval (%)	St, W St–W	S	SA An	Overall	Arithmetic mean	rms
HFM	0.206	±50	63	—	83	69	+41.0	112.4
		±30	50	—	75	54		
	0.5	±50	45	9	89	54	+61.2	127.2
		±30	20	9	79	40		
SFM	0.206	±50	100	—	83	95	−21.5	38.6
		±30	87	—	58	79		
	0.5	±50	85	64	84	80	−19.2	65.9
		±30	70	27	58	56		
RSM1	0.206	±50	60	—	100	71	+39.4	102.9
		±30	47	—	83	57		
	0.5	±50	55	27	79	58	+43.2	86.0
		±30	30	27	79	48		
RSM2	0.206	±50	60	—	83	67	+57.9	116.8
		±30	50	—	75	57		
	0.5	±50	35	18	74	46	+75.4	144.7
		±30	25	9	68	38		
HLM	0.206	±50	60	—	100	71	+42.3	104.3
		±30	50	—	83	60		
	0.5	±50	47	25	79	54	+54.7	108.9
		±30	26	8	79	50		

[a] HFM = homogeneous flow model, SFM = separated flow model, RSM1 = Reimann and Seeger (1986) model with $y = 1.0$, RSM2 = Reimann and Seeger (1986) model with $y = 1.34$, HLM = Hwang and Lahey (1988) model.

However, in the semi-annular and annular flow regimes the models by Reimann and Seeger (1986) (RSM1), Hwang and Lahey (1988) and the homogeneous flow model all perform better than the separated flow model. The model presented by Reimann and Seeger (1986) generally performed better when their correction factor, y, was set equal to 1.0 (RSM1) than when $y = 1.34$ (RSM2).

4. Concluding remarks

Phase-distribution and pressure-drop data were obtained for air–water flow in two reduced horizontal tee junctions where the main tube was 38.1 mm i.d. and the branch tubes were 19 mm i.d. and 7.85 mm i.d. These data extend the earlier results of Buell et al. (1994) taken from the same laboratory with an equal-sided tee junction. The present data were compared against existing correlations for phase distribution and pressure drop. Also, the present phase-distribution data were compared against data from previous investigations.

It was found that for $D_3/D_1 = 0.5$ most of the stratified, stratified–wavy, wavy and semi-annular data show a preference for the gas phase to exit through the branch. The slug-flow data displayed a strong preference of the gas phase to exit through the branch. The annular flow data showed large variations in the distribution of the phases depending on J_{L1}.

For $D_3/D_1 = 0.206$, the stratified, stratified–wavy, wavy and semi-annular data show a preference for the gas phase to exit through the branch at low extraction rates. In places where larger extraction rates could be obtained, the data showed a sudden change in trend with increasing proportions of liquid exiting through the branch.

The model by Azzopardi (1988) for predicting the phase-distribution data in the annular flow regime gave the best results for both diameter ratios. The model by Hart et al. (1991) also gave good results for the stratified, wavy and annular flow regimes.

For ΔP_{12}, the separated flow model (SFM) by Fouda and Rhodes (1974) gave the best overall predictions for both test sections and all inlet flow regimes, except slug flow. For ΔP_{13}, the separated flow model (SFM) proposed by Saba and Lahey (1984) gave the best overall predictions for both test sections. However, the homogeneous flow model (HFM) and the models by Reimann and Seeger (1986) (RSM1) and Hwang and Lahey (1988) (HLM) gave slightly better results in the semi-annular and annular flow regimes.

Acknowledgements

The financial support provided by the Natural Sciences and Engineering Research Council of Canada is gratefully acknowledged.

References

Azzopardi, B.J., 1988. An additional mechanism in the flow split of high quality gas–liquid flows at a T junction. UKAEA Report AERE-R 13058.

Azzopardi, B.J., Wagstaff, D., Patrick, L., Memory, S.B., Dowling, J., 1988. The split of two-phase flow at a horizontal T—annular and stratified flow. UKAEA Report AERE-R 13059.

Ballyk, J.D., 1992. Dividing annular/two-phase flow in horizontal T-junctions. Ph.D. thesis, McMaster University.

Ballyk, J.D., Shoukri, M., Chan, A.M.C., 1988. Steam–water annular flow in a horizontal dividing T-junction. International Journal of Multiphase Flow 14, 265–285.

Buell, J.R., 1992. Two-phase pressure drop and phase distribution in a horizontal tee junction. M.Sc. thesis, University of Manitoba.

Buell, J.R., Soliman, H.M., Sims, G.E., 1994. Two-phase pressure drop and phase distribution at a horizontal tee junction. International Journal of Multiphase Flow 20, 819–836.

Collier, J.G., 1976. Single-phase and two-phase behaviour in primary circuit components. In: Proc. NATO Advanced Study Institute on Two-Phase Flow and Heat Transfer, Istanbul, Turkey.

Fouda, A.E., Rhodes, E., 1974. Two-phase annular flow stream division in a simple tee. Transactions of the Institute of Chemical Engineers 52, 354–360.

Hart, J., Hamersma, P.J., Fortuin, J.M.H., 1991. Phase distribution during gas–liquid flow through horizontal dividing junctions. Nuclear Engineering Design 126, 293–312.

Henry, J.A.R., 1981. Dividing annular flow in a horizontal tee. International Journal of Multiphase Flow 7, 343–355.

Hwang, S.T., Lahey, R.T., 1988. A study on single- and two-phase pressure drop in branching conduits. Experimental Thermal and Fluid Science 1, 111–125.

Hwang, S.T., Soliman, H.M., Lahey, R.T., 1988. Phase separation in dividing two-phase flows. International Journal of Multiphase Flow 14, 439–458.

Kataoka, I., Ishii, M., 1983. Entrainment and deposition rates of droplets in annular two-phase flow. In: Proc. ASME/JSME Therm. Engng Joint Conf., Honolulu, Hawaii, Vol. 1, pp. 69–80.

Mandhane, J.M., Gregory, G.A., Aziz, K., 1974. A flow pattern map for gas–liquid flow in horizontal pipes. International Journal of Multiphase Flow 1, 537–553.

Reimann, J., Seeger, W., 1986. Two-phase flow in a T-junction with a horizontal inlet—part II: pressure differences. International Journal of Multiphase Flow 12, 587–608.

Reimann, J., Brinkmann, H.J., Domanski, R., 1988. Gas–liquid flow in dividing tee-junctions with a horizontal inlet and different branch orientations and diameters. Kernforschungszentrum Karlsruhe, Report KfK 4399.

Rouhani, Z., 1969. Modified correlations for void and two-phase pressure drop. AB Atomenergi Sweden, Report AE-RTV-841.

Rubel, M.T., Soliman, H.M., Sims, G.E., 1988. Phase distribution during steam–water flow in a horizontal T-junction. International Journal of Multiphase Flow 14, 425–438.

Saba, N., Lahey, R.T., 1984. The analysis of phase separation phenomena in branching conduits. International Journal of Multiphase Flow 10, 1–20.

Shoham, O., Brill, J.P., Taitel, Y., 1987. Two-phase flow splitting in a tee junction—experiment and modeling. Chemical Engineering Science 42, 2667–2676.

Shoham, O., Arirachakaran, S., Brill, J.P., 1989. Two-phase flow splitting in a horizontal reduced pipe tee. Chemical Engineering Science 44, 2388–2391.

Walters, L.C., 1994. Two-phase pressure drop and phase distribution at horizontal tee junctions: the effect of branch diameter. M.Sc. thesis, University of Manitoba.

Zuber, N., Findlay, J.A., 1965. Average volumetric concentration in two-phase flow systems. Journal of Heat Transfer 87, 453–468.